The predominance of one of the SR-BI isoforms is associated with increased esterified cholesterol levels not apoptosis in mink testis

Casimir D. Akpovi, Suk Ran Yoon, María Leiza Vitale, and R-Marc Pelletier[1]

Département de Pathologie et Biologie Cellulaire, Faculté de Médecine, Université de Montréal, Montréal, Québec, Canada

Abstract **Scavenger receptor class B type I (SR-BI) contributes to HDL-mediated cellular cholesterol efflux and is a phagocytosis-inducing phospholipid phosphatidylserine receptor in rat Sertoli cells, whereas the spliced variant of the SR-B gene, SR-BII, is implicated in the efflux of free cholesterol in macrophages. This study aimed to assess whether spontaneous autoimmune orchitis (AIO), which causes impaired clearance of apoptotic germ cells and spermatogenic arrest, involves SR-BI, SR-BII, and/or cholesterol. The levels measured during development and the annual reproductive cycle in normal mink were compared with those in mink with spontaneous AIO. Time periods with lowest tubular esterified cholesterol (EC) levels showed maximal SR-BI and SR-BII levels, and the periods when one or the other SR-BI isoform predominated showed increased EC levels and spermatogenic arrest in normal mink seminiferous tubules. In tubules with AIO, the predominance of only one or the other SR-BI isoform was the reverse of that measured in normal tubules, and it was associated with an increase in EC levels but not with apoptosis levels. SR-BI and SR-BII levels were not correlated with serum testosterone levels. SR-BI mainly localized to the Leydig cell, germ cell, and Sertoli cell surface, where its distribution was stage-specific. SR-BII was principally intracellular. Tubules from testes with AIO showed a deregulation of cholesterol homeostasis and SR-BI expression but relatively unchanged apoptosis levels. These results suggest that the expression of both SR-BI isoforms is required for the maintenance of low EC levels and that the predominance of only one isoform is associated with the accumulation of EC but not with apoptosis in the tubules.**—Akpovi, C. D., S. R. Yoon, M. L. Vitale, and R-M. Pelletier. **The predominance of one of the SR-BI isoforms is associated with increased esterified cholesterol levels and not with apoptosis in mink testis. *J. Lipid Res.* 2006.** 47: **2233–2247.**

Supplementary key words scavenger receptor class B type I • Sertoli cell • autoimmune orchitis • cell clearance • Leydig cell

The report of a high incidence of dyslipidemia in infertile men (1) is one of a body of evidence that cholesterol is indispensable for gamete development and fertility (2–8). The source of cholesterol for Leydig cells is de novo synthesis and HDL, one of several lipoproteins transporting lipids from blood (9–11). In the seminiferous tubules, the other compartment of the testis, the basement membrane, which separates each tubule from blood capillaries, blocks LDL while allowing the entry of HDL (11), the major source of cholesterol for Sertoli cells (12). In addition, the blood-testis barrier formed by junctional complexes joining Sertoli cells (13, 14) has been said to be opposed to the entry of circulating cholesterol into the tubules (15). Although Sertoli cells show the capacity to synthesize cholesterol from acetate in vitro (16), there is no evidence that they do so in large amounts in vivo. Besides the blood circulation, cholesterol within the tubules themselves originates from the phagocytosis of lipid-containing residual bodies, lipid-rich cells, and apoptotic germ cells or their cell membrane remnants, which can represent up to 50% of cell loss in normal testis (17, 18). The observation that free cholesterol (FC) concentration in the interstitial tissue equals that in tubules (19, 20) entails factors regulating cholesterol influx and efflux to maintain equilibrium.

The nonenzymatic factors potentially involved in cholesterol homeostasis include ABCA1, which transfers cholesterol to apolipoprotein 1 (7, 21), and CD36 (22), which mediates the selective uptake of HDL cholesteryl esters and binds oxidized low density lipoproteins. In addition, scavenger receptor class B type I (SR-BI) selectively removes cholesteryl esters from the HDL to which it binds (23, 24) and contributes to the HDL-mediated cellular cholesterol efflux (25). Moreover, SR-BI is highly expressed in tissues with a strong cholesterol demand for steroidogenesis, such as adrenals, ovaries, and testes (23, 24). Experimental deficiency of SR-BI is accompanied by abnormal structure, composition, and abundance of lipoproteins, which alters the development of female gametes and

Manuscript received 10 April 2006 and in revised form 7 July 2006.

Published, JLR Papers in Press, July 21, 2006.
DOI 10.1194/jlr.M600162-JLR200

[1] To whom correspondence should be addressed.
e-mail: marc.pelletier@umontreal.ca

causes a significant proportion of ovulated oocytes to die soon after ovulation, resulting in sterility in *SR-B* gene-knockout female mice (26). SR-BII, a spliced variant of the *SR-B* gene that differs from SR-BI only in the C-terminal cytoplasmic domain, also binds HDL with high affinity (27). In contrast to SR-BI, SR-BII does not mobilize intracellular cholesteryl ester stores and is less efficient at promoting cellular cholesterol efflux (27), but it effluxes 2-fold more FC than SR-BI in macrophages (28). Nonetheless, SR-BI and SR-BII both colocalize with cholesterol-rich plasma membrane caveolae (28–31), which influence cholesterol homeostasis by acting as conduits for cellular flux (32) and concentrate signaling proteins for signal transduction (33).

Autoimmune orchitis (AIO) is characterized by an increase in serum anti-sperm antibody levels, inflammation of the testis, leukocyte infiltration, degeneration of the germinal epithelium, spermatogenic arrest, and infertility (34). Spontaneous AIO has been documented in human, dog, mink, and rat (35). The incidence of inflammation of the testis is high in infertile males, and testicular inflammation has been identified as a cause of infertility, although symptomatic orchitis caused by bacterial or viral infections is a rare occurrence in men (36). Immunological male infertility is associated with pathological features that resemble granulomatous orchitis, with inflammation of the testis and persistent infertility documented in infertile mink with spontaneous AIO (35). To assess whether testicular SR-BI, SR-BII, esterified cholesterol (EC), and FC were affected by an impaired clearance of apoptotic germ cells caused by AIO, measurements performed in mink with spontaneous AIO were compared with those in normal development and the annual reproductive cycle. The model provides a unique opportunity to highlight the relationship between apoptosis, germ cell removal, SR-BI expression, and cholesterol levels. This information is significant because injection of a part of the extracellular domain of rat SR-BI fused with human FC in the tubules was claimed to cause an increased numbers of apoptotic germ cells (37) and because phagocytosis of apoptotic germ cells by Sertoli cells was said to be mediated by SR-BI in rodents (31, 37–39).

This study shows that the time periods during the annual seasonal reproductive cycle characterized by high levels of SR-BI and SR-BII were accompanied by low EC levels in the tubules, whereas the periods characterized by the predominance of one of the two SR-BI isoforms were accompanied by high EC levels. These results show that tubules with AIO were characterized by a deregulation of cholesterol homeostasis and a concurrent deregulation of SR-BI and SR-BII expression. This study also shows that an increase in only one of the two SR-BI isoforms in the tubules with AIO was accompanied by increased EC levels but not by a significant increase in apoptosis levels, suggesting that the recognition and phagocytosis of apoptotic cells are distinct physiological events and that the engulfment of apoptotic cells by Sertoli cells is only partly dependent on SR-BI.

MATERIALS AND METHODS

Animals

All mink (*Mustela vison*) purchased from Visonnière St. Damase (St. Damase, Québec, Canada) were individually caged, fed a high-protein diet, kept under natural lighting conditions, and allowed food and water ad libitum. After anesthesia by intraperitoneal injection of 0.9 ml/kg body weight sodium phenobarbital (Somnotol; MCI Pharmaceutical, Mississauga, Ontario, Canada) and 0.15 ml/kg body weight of a solution of 0.3 g/ml chloral hydrate in sterile saline, mink were decapitated and the trunk blood and tissues were collected. For studies on development, testes were harvested at 30 day intervals *1*) during the neonatal period (60–90 days old), *2*) during puberty (120, 150, 210, and 240 days old), and *3*) by the onset of adulthood (270 days old). Adult mink testes were collected at 30 day intervals during the last week of the month throughout the annual reproductive cycle from 1–2 year old mink. The calendar of the monthly changes in germ cell population during the annual reproductive cycle and the method of Pelletier (40) for the identification of the 12 stages of the cycle of the seminiferous epithelium were used. Six normal mink per age group were used except when testes were small during puberty, when 6–10 mink were used.

For studies on infertile male mink, 2–3 year old mink that successfully mated and sired five litters of no fewer than four kits the year before but that were sterile during the current year and were diagnosed with spontaneous AIO were selected.

Clinical criteria of fertility

The ejaculated semen recovered from vaginal smears was evaluated with a light microscope, and the morphology, motility, and number of spermatozoa were assessed for each male mink during the mating season in March. For studies in infertile mink, those that failed to sire a litter, whose semen contained low counts of spermatozoa, immobile spermatozoa, or no spermatozoa with high serum levels of anti-sperm antibodies, and whose pathological features showed leukocyte infiltration and destruction of the seminiferous epithelium at autopsy typical of spontaneous AIO were used. Ten adult mink with AIO for February, March, and July (totaling 30 mink) were used. The right testis was processed for histological studies and the left for enriched tissue fractionation. The protocol was approved by the Université de Montréal Animal Care Committee.

Quantification of serum anti-sperm antibodies by ELISA

The methods of Ing et al. (41) and Benet-Rubinat et al. (42) were used as follows. One hundred microliters of spermatozoa suspended in PBS (137 mM NaCl, 3 mM KCl, 8 mM Na_2HPO_4, and 1.5 mM KH_2PO_4, pH 7.4) at a concentration of 1×10^6 cells/ml was added to each well (1×10^5 cells/well) of polystyrene flat-bottom plates (Immulon 2; Dynex Technology, Chantilly, VA), and the plates were centrifuged at 2,000 rpm in a GS-6R Beckman centrifuge (Beckman, Mississauga, Ontario, Canada) equipped with a GH 3.8 rotor at 4°C for 10 min. The supernatant was removed and the plates were dried. Spermatozoa were fixed in −20°C methanol for 30 min, dried, incubated with 1% BSA in PBS at 4°C overnight to eliminate nonspecific labeling, and washed in PBS containing 0.05% Tween 20. Spermatozoa were incubated first with various dilutions of mink sera (higher dilutions were needed when sera of infertile mink were used). Serum dilutions were prepared in 1% BSA in PBS ranging from 1:100 to 1:1,000. Spermatozoa were incubated with serum dilutions at 37°C for 1 h, next with rabbit anti-mink IgG (1:2,000 dilution) at 37°C for 1 h, and then with HRP-conjugated anti-rabbit IgG (1:2,000 dilution) at 37°C for 1 h. The reaction was detected by adding

100 μl of substrate solution containing 0.4 mg/ml orthophenylene diamine and 0.015% hydrogen peroxide in citrate buffer, pH 5.0, and stopped by the addition of 25 μl/well of 2 N sulfuric acid. Optical density was determined at 492 nm by an ELISA autoreader (Dynatech, Mississauga, Ontario, Canada). All samples were assayed in duplicate, and the results are expressed as fold dilution of serum where the absorbance value was 0.5.

Isolation of seminiferous tubule- and interstitial tissue-enriched fractions

Testes were decapsulated and immersed in PBS with or without phosphatase and protease inhibitors: 2 mM PMSF, 1 mM EGTA, 2 μg/ml leupeptin, 2 μg/ml aprotinin, 4 mM Na_3VO_4, 80 mM NaF, 20 mM $Na_4P_2O_7$, and 10 μM potassium bisperoxol-(1,10-phenanthroline)oxovanadate. The seminiferous tubules were teased apart and individually detached from the interstitial tissue with fine tweezers. Next, the tubule-interstitial tissue mixture was placed in PBS with or without phosphatase inhibitors in a water shaker bath set at 80 cycles/min at 4°C for 1 h. The mixture was allowed to sediment for 1 h in 15 ml conical tubes on ice and centrifuged at 600 rpm for 20 min in a GS-6R Beckman centrifuge equipped with a GH 3.8 rotor at 4°C. The seminiferous tubule-enriched fraction (STf) occupied the pellet, and the interstitial tissue fraction (ITf) occupied the top. The fractions were washed in PBS or PBS containing proteases and phosphatase inhibitors, and their purity was evaluated by light microscopy. This represents a modification of a previously published isolation method in which mild enzymatic digestion with collagenase D and soybean trypsin inhibitor was used to separate tubules from the interstitial tissue (19). The protein content of the ITf and STf samples was measured (43).

Quantification of apoptosis by ELISA

Measurements were done using a cell death detection ELISA kit (Boehringer-Mannheim, Laval, Québec, Canada) in accordance with the manufacturer's instructions. The assay kit allows the quantification of mononucleosome- and oligonucleosome-bound DNA in the cytoplasmic fraction of a cell homogenate that is caused by DNA fragmentation during apoptosis. Briefly, STf homogenates were incubated with the lysis buffer at room temperature for 30 min and centrifuged at 15,000 rpm in a Beckman centrifuge (Palo Alto, CA) at 4°C for 30 min. The cytosolic fractions were collected, and 20 μg of proteins was loaded onto streptavidin-coated microtiter plates, exposed to anti-histone biotin and peroxidase-conjugated anti-DNA antibody at room temperature for 2 h, washed, and incubated with 2,2′-azino-di-[3-ethylbenzithiazoline sulfonate] diammonium salt substrate solution. The results are expressed in absorbance unit per milligram of protein STf (AU/mg). Samples were assayed in duplicate.

Epididymal spermatozoa

Epididymides from normal adult mink euthanized in February and March were diced in cold PBS with or without proteases and phosphatase inhibitors, filtered through a 74 μm mesh, and centrifuged at 2,000 rpm for 15 min in a GS-6R Beckman centrifuge at 4°C to recover spermatozoa. The gametes were resuspended in 10 mM Tris-HCl, pH 8, containing 1 mM EDTA for 5 min to lyse epithelial and blood cells (44), washed twice, and diluted 1:1 in cold PBS with or without proteases and phosphatase inhibitors. The cells were sonicated in a Fisher Sonic Dismembrator (model 300; Fisher, Farmington, NY) during three 30 s intervals.

Antibodies against SR-BI and SR-BII

Three distinct antibodies were used for the detection of SR-BI and its isoform SR-BII: *1*) the polyclonal antibody to SR-BI, which recognizes only the SR-BI isoform, was raised in rabbit against a peptide antigen corresponding to residues 496–509 of mouse SR-BI; *2*) the goat polyclonal antibody to SR-BI produced against a synthetic peptide made to the C-terminal region of murine SR-BI, corresponding to residues 400–509; and *3*) the rabbit polyclonal antibody, which recognizes exclusively the SR-BII isoform, was produced against a peptide antigen corresponding to residues 491–506. In addition, the rabbit SR-BII antibodies were affinity-purified against the recombinant SR-BII coupled to a CNBr-activated Sepharose 4B column. Antibodies 1 and 3 above were purchased from Novus Biologicals (Littleton, CO). The goat polyclonal antibody to SR-BI was a generous gift from Novus Biologicals. The affinity-purified antibodies are specific for each isoform of SR-BI and do not cross-react with other proteins in Western blot analyses of tissue extracts. The specificity of SR-BI and SR-BII antibodies was tested using mouse tissue as a positive control. The primary or secondary antibody alone was used for negative controls.

Electrophoresis and Western blots

Twenty micrograms of total proteins for each STf and/or ITf sample was denatured in electrophoresis sample buffer and loaded on a 10% polyacrylamide minigel, subjected to electrophoresis, and electrotransferred onto nitrocellulose membranes. Membranes blocked for 60 min at 37°C with 5% skim milk in TBS (140 mM NaCl and 50 mM Tris-HCl, pH 7.4) were incubated with purified anti-SR-BI (1:2,000 dilution) or anti-SR-BII (1:1,000) overnight and mixed with the corresponding HRP-conjugated secondary antibody. Some membranes were reprobed with either a goat polyclonal antibody to human vimentin (Sigma, St. Louis, MO) (1:500 dilution) or a monoclonal anti-human clusterin (Novocastra Laboratories, Ltd., New Castle upon Tyne, UK) (1:50 dilution).

For studies of AIO, myosin light chain (MLC) was used as an internal loading control. MLC has a molecular mass of 20 kDa, and the intensity of the band did not change in the different experimental conditions. The membranes between 40 and 50 kDa were incubated with monoclonal MLC antibody (Sigma) and then with anti-IgM peroxidase-conjugated antibody. Antigen-antibody complexes were revealed using enhanced chemiluminescence (Lumi-light$^+$; Roche, Laval, Québec, Canada).

Plasma and testicular cholesterol analysis

Duplicate samples of enriched tissue fraction homogenates (60–80 μl each) and serum (40–60 μl) were extracted with 5 ml of hexane-isopropanol (3:2) for 30 min at room temperature and centrifuged at 2,500 rpm (GS-6R Beckman centrifuge) for 5 min (45). The supernatant was removed, and the extraction was repeated three times on the pellet. The supernatant from each sample was pooled, separated into two equal volumes, and evaporated at 37°C with N-EVAP Nitrogen Evaporators (Organomation Associates, Inc., Berlin, MA). Total cholesterol (TC) and unesterified FC were measured in the dried pellet from the 2 volumes with an enzymatic kit (Wako Chemical USA, Inc., Richmond, VA). EC levels were obtained by substraction of FC from TC. EC and FC contents are expressed in μg cholesterol/mg total protein for ITf and STf or in mg cholesterol/dl serum. The values are means ± SEM from three independent experiments.

Immunolabeling

Testes were perfusion-fixed with Bouin's fixative (46). Endogenous peroxidase activity was inhibited with 0.3% hydrogen peroxide, and immunolabeling was performed (19). Nonspecific binding was blocked with 0.5–3.0% skim milk. Paraffin sections were incubated with rabbit anti-SR-BI (1:50 dilution), goat anti-SR-BI (1:100 dilution), or rabbit anti-SR-BII (1:25 dilution), then

with biotinylated anti-rabbit F(ab′)$_2$ (1:10,000 dilution) or anti-goat IgG (1:2,000 dilution) and peroxidase-conjugated streptavidin (1:200 dilution) (20). Controls included either the first or the second antibody alone.

Fluorescence microscopy

Spermatozoa mounted on poly-L-lysine-coated cover slips were air-dried, fixed, and permeabilized with −20°C methanol for 10 min. Preparations were incubated with 3% skim milk in PBS to block nonspecific binding. Next, spermatozoa were incubated with purified anti-SR-BI (1:10 dilution) or anti-SR-BII (1:5 dilution) for 60–120 min at 37°C, rinsed with PBS, and incubated with FITC-conjugated anti-rabbit IgG (1:400 dilution) at 37°C for 1 h. Cover slips were mounted in PBS/glycerol (1:1) containing 5% 1,4-diazabiscyclo-[2,2,2]octane and visualized with a Carl Zeiss Axioskop II fluorescence microscope.

Measurements of serum testosterone levels

Testosterone concentration in mink sera was measured by ELISA using ALPCO diagnostics kits (American Laboratory Products Company, Salem, NH) (19). The sensitivity of the method was 0.07 ng/ml.

Data analysis and statistical analysis

The bands of five independent immunoblots of SR-BI and SR-BII obtained for each time interval studied in ITf and STf were scanned on an Astra 2000S laser scanner (Umax Data System, Inc., Hainchu, Taiwan). The relative SR-BI and SR-BII protein contents of scanned bands were estimated by densitometry (Scion Image Software, Scion Corp.). The values were normalized to 60 day values for the studies of development or to August values for the studies of adults. The data are presented as means ± SEM and were evaluated with Student's *t*-test.

Source of chemicals and antibodies

Poly-L-lysine and 1,4-diazabiscyclo-[2,2,2]octane were from Sigma-Aldrich (Oakville, Ontario, Canada), and PMSF, biotinylated anti-rabbit IgG, biotinylated anti-goat IgG, leupeptin, aprotinin, and the Lumi-light$^+$ chemiluminescence detection kit were from Roche. Potassium bisperoxol-(1,10-phenanthroline) oxovanadate(V) was from Calbiochem (San Diego, CA). Biotinylated anti-rabbit affinity-purified F(ab′)$_2$ fragment and peroxidase-conjugated anti-rabbit IgG, peroxidase-conjugated anti-mouse IgG, and anti-goat IgG were purchased from Jackson Immunoresearch Laboratories (Mississauga, Ontario, Canada).

RESULTS

In the mink, the neonatal period covers the first 90 days after birth, generally by May in the northern hemisphere, and it is followed by puberty, which lasts from day 91 to day 252 after birth. Spermatogenesis is completed by day 240 after birth. The appearance of spermatozoa in the epididymis 12 days later in January is the hallmark for the onset of adulthood (40). The annual seasonal reproductive cycle in the adult is composed of an 8 month long active spermatogenic phase, beginning with the division of spermatogonial stem cells in August and ending with the arrest of spermatogenesis by the last week of March. Spermatozoa are produced from January to March (40). This is followed by a 4 month long inactive spermatogenic phase, or testicular regression, from April until the end of July (40). The duration of the cycle of the seminiferous epithelium lasts 58 days in mink (47).

Western blot analyses of SR-BI and SR-BII in mink and mouse tissue fractions

When anti-SR-BI was used, one immunoreactive band was detected in the ITf and one in the STf (**Fig. 1**). Although the molecular mass was the same in both mink tissue fractions, the mass was 82 kDa in mink and 85 kDa in mouse (Fig. 1). Anti-SR-BII showed a molecular mass of 85 kDa in the two tissue fractions in both species (Fig. 1).

Western blot analyses of SR-BI and SR-BII in mink tissues

The intensity of the SR-BI immunoreactive band was strongest in mink ITf followed by the liver, STf, kidney, small intestine, and lung. The heart and brain contained traces (**Fig. 2A**). The intensity of the SR-BII immunoreactive band was strongest in the ITf and next in the STf and kidney (Fig. 2B). Contrary to SR-BI, the liver and small intestine contained only traces of SR-BII (Fig. 2B).

Measurements of SR-BI and SR-BII levels in the ITf

During development, SR-BI levels increased from 90 to 180 days, then leveled off until 270 days (Fig. 2C). During the annual cycle, SR-BI levels decreased significantly by March, leaving traces from April to June, but increased significantly by July and stayed high from August until February (Fig. 2D).

During development, traces of SR-BII were detected from 60 to 120 days, but the levels increased significantly from 120 to 150 days, from 150 to 180 days, and from 210 to 240 days (Fig. 2E). In contrast to SR-BI (Fig. 2D), SR-BII levels were low from July to October but high from November to June (Fig. 2F). SR-BII levels increased significantly from October to November (Fig. 2F) but decreased from June to July (Fig. 2F).

Measurements of SR-BI and SR-BII levels in the STf

During development, SR-BI levels increased significantly from 120 to 150 days, when they peaked and reached values

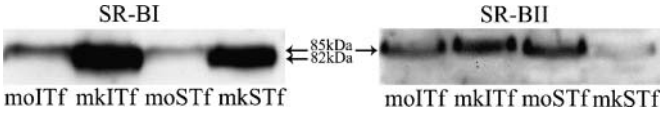

Fig. 1. Specificity of anti-scavenger receptor class B type I (SR-BI) and anti-SR-BII antibodies in mink and mouse seminiferous tubule-enriched fraction (STf). Representative Western blots show one immunoreactive band of 82 kDa in interstitial tissue fraction (ITf) (mkSTf) and STf (mkSTf) from adult mink in February, when anti-SR-BI antibodies were used. In mouse ITf (moITf) and STf (moSTf), the band shows a molecular mass of 85 kDa with the same antibodies. When SR-BII antibodies were used on the same samples, the immunoreactive band detected had a molecular mass of 85 kDa in the ITf and STf of both species.

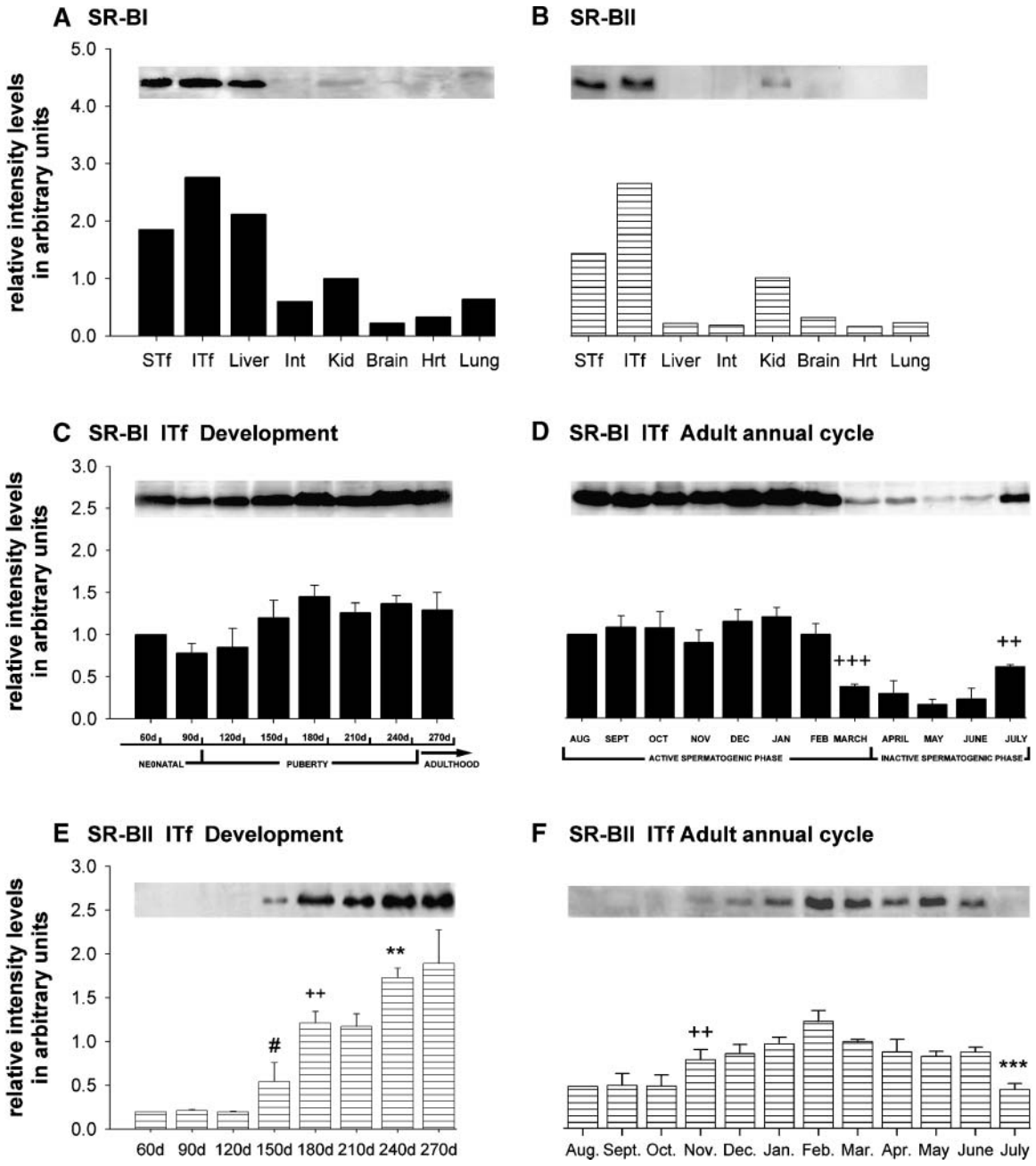

Fig. 2. Assessment of SR-BI and SR-BII levels in mink tissues and in the ITf during development and the annual reproductive cycle. A: Representative Western blot analysis of SR-BI showing that the molecular mass of SR-BI was 82 kDa in all of the mink tissues assayed. The histogram shows SR-BI protein levels expressed in arbitrary units. The SR-BI levels were highest in ITf followed by STf, liver, kidney (Kid), lung, and small intestine (Int). The brain and heart (Hrt) contained traces of the protein. B: Representative Western blot analysis of SR-BII. The intensity of the 85 kDa immunoreactive band was strongest in the ITf followed by the STf and kidney. Weak traces of the protein were present in the lung, small intestine, brain, and heart. The SR-BII protein levels are expressed in arbitrary units. C, D: Western blot analyses of SR-BI in ITf obtained monthly throughout development (C) and during the seasonal annual reproductive cycle in the adult (D). Representative Western blots show that the 82 kDa SR-BI-immunoreactive band is detected throughout both development and the annual reproductive cycle in the adult. The intensities of the bands obtained in six independent experiments were normalized to the 60 day data for development or to the August data for the annual reproductive cycle. The values shown are means ± SEM. $^{+++}$ $P < 0.00001$, February versus March; $^{++}$ $P < 0.001$, June versus July. E, F: Representative Western blot analyses of SR-BII in the ITf obtained monthly during development (E) and throughout the annual reproductive cycle (F). The intensities of the bands obtained in six independent experiments were normalized to the 60 day data for development or to the August data for the annual cycle. The values shown are means ± SEM. $^{\#}$ $P < 0.02$, 120 versus 150 days; $^{++}$ $P < 0.001$, 150 versus 180 days; ** $P < 0.005$, 210 versus 240 days ***$P < 0.00005$.

that neared twice the ITf values before decreasing until 270 days; the decrease was significant between 180 and 210 days (**Fig. 3A**). During the annual reproductive cycle, SR-BI levels were increased by August, then they decreased significantly by September before increasing again to reach peak values until February (Fig. 3B). From February to March, there was a very significant decrease in SR-BI levels, and only traces of the receptor were detected from April to June. However, this was followed by a significant increase in SR-BI levels from June to July (Fig. 3B). SR-BI was detected in epididymal spermatozoa isolated from adult mink in February and March (Fig. 3B).

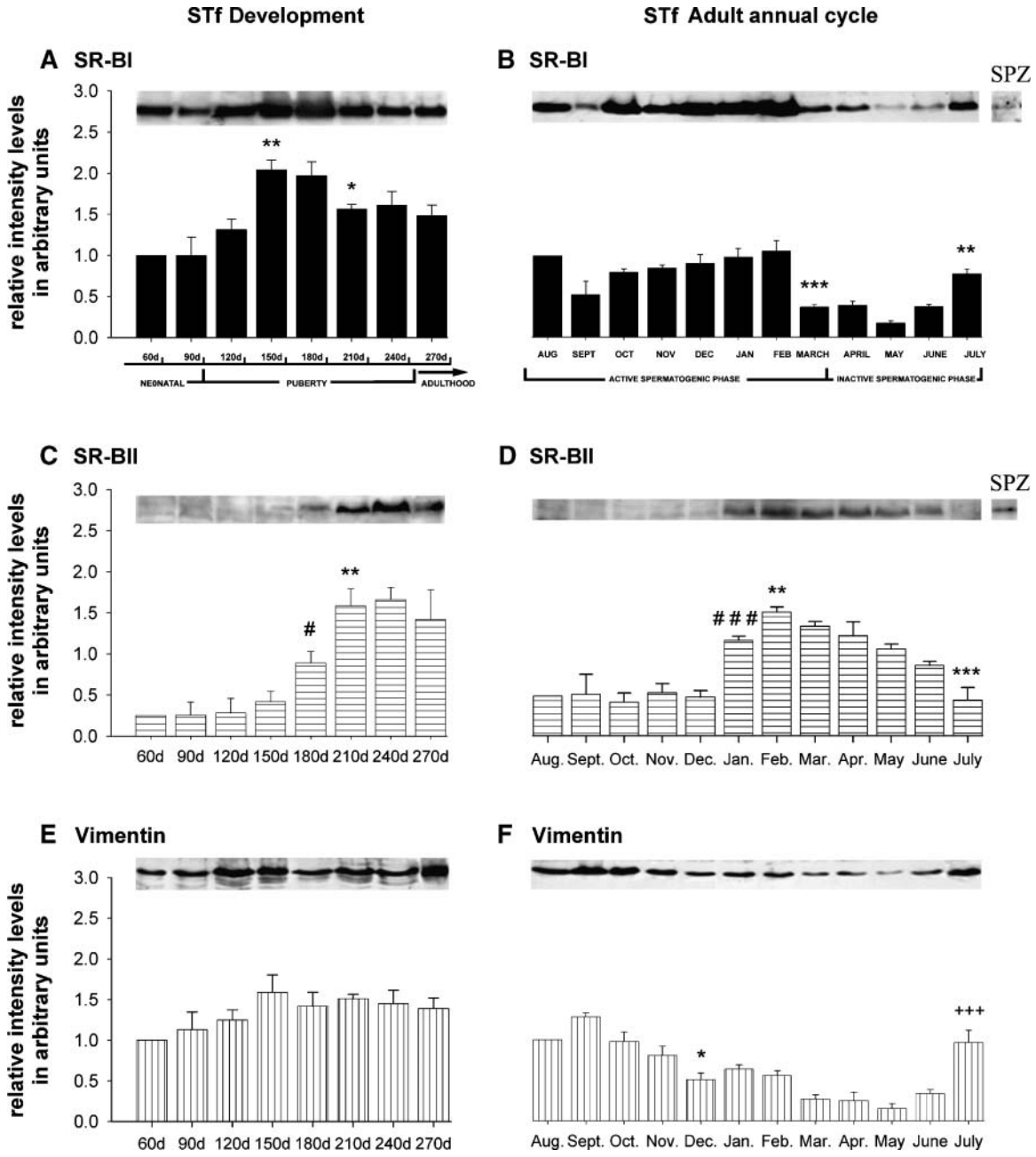

Fig. 3. Measurements of SR-BI and SR-BII levels and of vimentin in the STf during development and the annual reproductive cycle. A, B: Representative Western blot analyses of SR-BI in the STf obtained monthly during development (A) and the annual reproductive cycle (B) and in epididymal spermatozoa (SPZ). * $P < 0.05$, 180 versus 210 days and August versus September; ** $P < 0.005$, 120 versus 150 days and June versus July; *** $P < 0.00005$, February versus March. C, D: Representative Western blot analyses of SR-BII in the STf obtained monthly during development (C) and the annual reproductive cycle (D) as well as in epididymal spermatozoa. $^{\#}$ $P < 0.02$, 150 versus 180 days; $^{\#\#\#}$ $P < 0.00002$, December versus January; ** $P < 0.005$, 180 versus 210 days and January versus February; *** $P < 0.00005$, June versus July. E, F: Representative Western blot analyses of vimentin performed on the same membranes for which the Western blots of SR-BI had been done. * $P < 0.05$, November versus December; $^{+++}$ $P < 0.00001$, June versus July. The intensity of the bands obtained in six independent experiments was measured to generate histograms, and values were normalized to the 60 day data for development or to the August data for the annual cycle. All values shown are means ± SEM.

During development, in contrast to SR-BI (Fig. 3A), there were only traces of SR-BII from 60 to 150 days, and the first significant increase in SR-BII occurred from 150 to 180 days (Fig. 3C). This 150–180 day SR-BII increase (Fig. 3C) was roughly concomitant with a decline in SR-BI levels in the STf (Fig. 3A). A second significant SR-BII increase occurred from 180 to 210 days (Fig. 3C). During the annual reproductive cycle, in contrast to SR-BI (Fig. 3B), SR-BII appeared in traces from August to December (Fig. 3D). The SR-BII levels were very significantly increased from December to January and again from January to February before decreasing from July to December (Fig. 3D). The SR-BII decrease was significant from June to July, and this (Fig. 3D) was concomitant with a significant SR-BI increase in July (Fig. 3B). Thus, SR-BII and SR-BI levels were inversely related to each other in the STf except for during the months of January and February. SR-BII levels were increased when the number of germ cells was high from January to June (Fig. 3D), suggesting that SR-BII is chiefly associated with germ cells and SR-BI is chiefly associated with Sertoli cells and germ cells. Spermatozoa contained SR-BII (Fig. 3D).

The immunoblot membranes used to measure SR-BI expression in the STf were stripped and reprobed for vimentin (Fig. 3E, F) and clusterin (data not shown because clusterin and vimentin variations were similar). The vimentin levels showed a profile of variations (Fig. 3E, F) reminiscent of that of SR-BI (Fig. 3A, B) but not SR-BII (Fig. 3C, D), suggesting that SR-BI is associated partly, albeit not exclusively, with Sertoli cells. This observation adds further support to the contention that SR-BII is principally associated with germ cells, because vimentin and clusterin have been considered to be normally synthesized by Sertoli cells, not germ cells.

Immunohistochemical studies of SR-BI

SR-BI localized to germ cells and Sertoli cells in a stage-specific manner in adult mink testes harvested in February (**Fig. 4A–D**). SR-BI localized at the surface of the thin Sertoli cell cytoplasmic processes surrounding the germ cells during stage I (Fig. 4A). By stages VII and VIII, intercellular Sertoli cell junctional membranes in the vicinity of spermatocytes near the basal third of the epithelium (Fig. 4B, C) and the "trunk" of the supporting cells were labeled (Fig. 4D). The cell surfaces in the intercellular clefts between zygotene spermatocytes and Sertoli cell as well as those between adjoining Sertoli cell processes were SR-BI-positive during stage X (Fig. 4D). Stage X is concomitant with the spermatocyte migration from the basal to the lumenal compartment in mink. SR-BI-positive material was detected at the germ cell's surface and within the cytoplasm, where it appeared as SR-BI-positive minute dots (Fig. 4A–D). Intracellular SR-BI-positive clumps were present in apoptotic germ cells (Fig. 4B). SR-BI localized to the Leydig cell surface (Fig. 4E).

The histological changes during puberty are similar to those of the testicular regression in reverse sequence in mink testis (40). Because changes in SR-BI immunolocalization during puberty during testicular regression were similar, only data recorded during the later period are presented here (Fig. 4F–H). SR-BI-positive dots were detected within the Sertoli cells' trunk (Fig. 4F), but cytoplasmic labeling decreased during testicular regression (Fig. 4H). In addition, the cell surface of Sertoli cells and germ cells was labeled; Sertoli cell membrane segments facing degenerating germ cells were intensely labeled (Fig. 4F–H). Sertoli cells contained large SR-BI-positive vacuoles after germ cells had been cleared from the tubules (Fig. 4G). Intracellular SR-BI-positive clumps were observed in germ cells undergoing apoptosis (Fig. 4F–H).

Immunohistochemical studies of SR-BII

Most SR-BII was detected intracellularly in the vicinity of the nucleus in germ cells (**Fig. 5A, B**) and Sertoli cells (Fig. 5A) in adult mink testes harvested in February, but this distribution did not change with the stage of the cycle (Fig. 5A, B). In addition, intercellular clefts between Sertoli cells and germ cells were weakly immunostained during stage X (Fig. 5B). The endothelial cells of blood vessels and other interstitial cells, but not Leydig cells, were SR-BII-positive (Fig. 5C). During testicular regression, the Sertoli cell surface was very weakly SR-BII-immunoreactive, although the immunoreactivity in this location was increased by May and June (cf. Fig. 5D, E with Fig. 5F). In addition, the intracellular immunoreactivity of SR-BII was localized to germ cells, in particular round spermatids and cells that showed signs of apoptosis (Fig. 5A). The protein was not detected in the interstitial space during testicular regression (Fig. 5D–F).

Immunofluorescence studies on epididymal spermatozoa

Spermatozoa incubated with the second antibody alone showed occasional nonspecific weak staining of the mitochondrial sheath in the tail (**Fig. 6A**). Scattered SR-BI-positive clumps covered the anterior acrosomal segment, and the mitochondrial sheath was labeled (Fig. 6B). SR-BII localized to the anterior acrosomal segment but more intensely than SR-BI in the same region, and the mitochondrial sheath was not labeled (Fig. 6C).

Measurements of FC and EC levels in the ITf and STf and serum

The developmental and seasonal FC and EC level variations in the ITf, STf, and serum are shown in **Fig. 7**. In the ITf, during development, FC levels reached a plateau at ~45 μg cholesterol/mg protein by 120 days until adulthood. Conversely, the increase in EC levels from 90 to 150 days was followed by a significant decrease ($P < 0.01$, 150 vs. 180 days old) by 180 days. In adult mink, FC levels were approximately three times the EC values. FC and EC levels were lower during the periods when spermatogenesis was completed (from December to March) than when it was not (the rest of the annual reproductive cycle). In the STf, FC values were three times the EC values. During development, FC levels showed no significant changes but EC levels decreased, although not significantly, until adult-

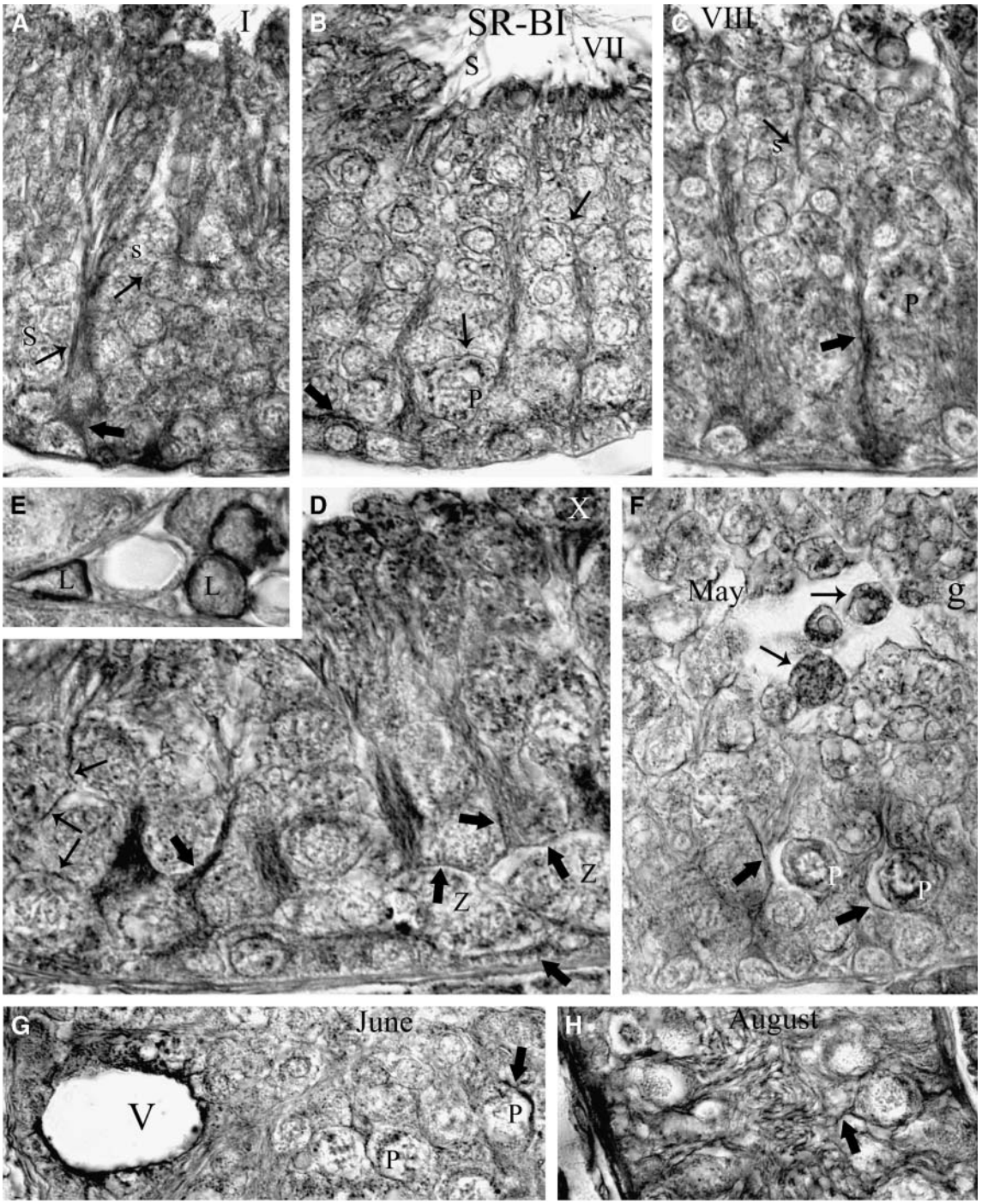

Fig. 4. Immunolocalization of SR-BI in adult mink testis. A–D: The stages of the cycle of the seminiferous epithelium appear in roman numerals at the top of the panels. SR-BI-positive dots are identified in germ cells. P, pachytene spermatocytes; s and S, rounded (s) and elongated (S) spermatids; Z, zygotene spermatocytes. In B, a pachytene spermatocyte showing signs of apoptosis contains clumps of SR-BI-positive material. In addition, the protein localizes at the surface of germ cells (thin arrows). In the Sertoli cell's cytoplasm, SR-BI labeling is abundant near the basal third of the epithelium (thick arrows in A–D). In addition, the localization of the protein coincides with the localization usually agreed to be that of the cell junctions within the Sertoli cell junctional complexes (thick arrows in B–D). Labeling in this location of the seminiferous epithelium is particularly intense during stage X of the cycle (D). It is apparent in the intercellular cleft separating zygotene spermatocytes from the neighboring Sertoli cells (the three thick arrows near the lowest zygotene spermatocytes in D) and in the clefts between adjacent Sertoli cells (the thick top right arrow in D and the thick arrow in C). Magnification, ×1,310. E: Within the interstitial tissue, SR-BI immunoreactivity was detected on the Leydig cell surfaces (L). Magnification, ×1,100. F: A tubule with a lumen in May. g, giant cell. G, H: Tubules with a collapsed lumen in June and August, respectively. SR-BI labeling is visible at the surface [thick arrows in F–H and along the outline of the large vacuole (V) in G] and in the Sertoli cell's cytoplasm principally near the basal third of the epithelium (thick arrows) and at the germ cell surface (P in F, G). SR-BI-positive clumps are identified in apoptotic germ cells (P in F, G and thin arrows in F). Magnification, ×780.

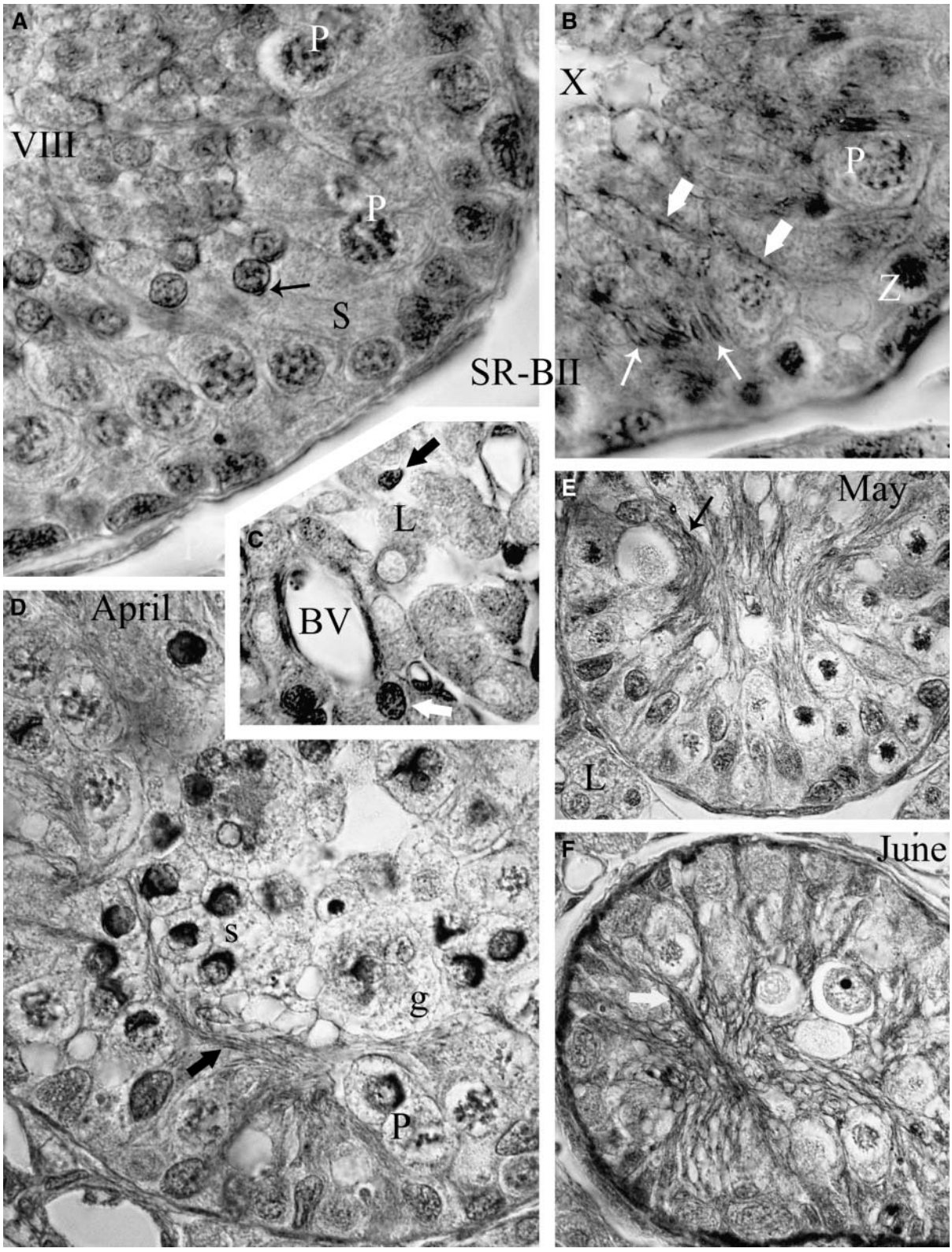

Fig. 5. Immunolocalization of SR-BII in adult mink testis. A, B: The stages of the cycle of the seminiferous epithelium appear in roman numerals at the top of the panels. SR-BII localizes to pachytene (P) and zygotene (Z) spermatocytes, round and elongated spermatids (thin arrows), and Sertoli cells (S). Labeling is visible near the nucleus (A, B) and at the Sertoli cell-germ cell interface (thick arrows in B). C: In the interstitial tissue, endothelial cells in blood vessels (BV) and interstitial cells (thick arrows) resembling macrophages are immunostained, but Leydig cells (L) are not. D: A tubule with a lumen in April. E, F: Tubules with a collapsed lumen in May and June, respectively. SR-BII labeling is weak at the surface of Sertoli cells, but immunoreactivity in this location is increased by May and June (thin arrows in D–F). SR-BII-positive material is detected in germ cells, particularly round spermatids showing signs of degradation; some spermatids are gathered into giant cells (g) and disposed like a plug in the reduced lumen (D). In June, the base of Sertoli cells is SR-BII-positive (F). Magnifications, ×1,000 (A, C); ×880 (B); ×1,190 (D); ×880 (E, F).

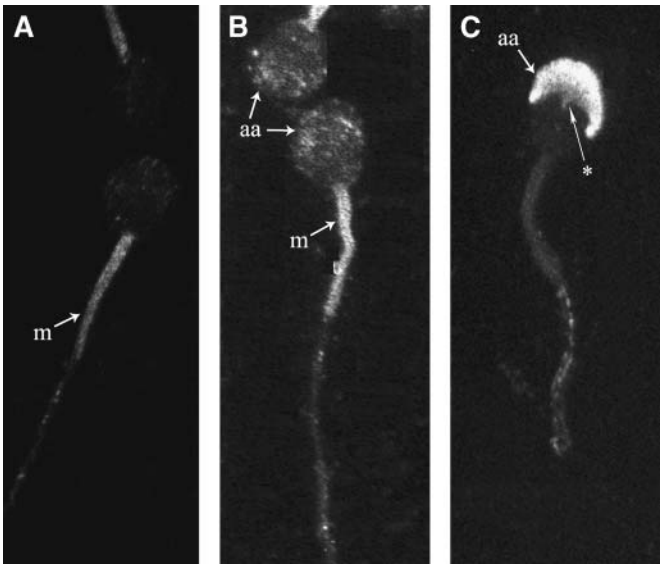

Fig. 6. Immunofluorescence localization of SR-BI and SR-BII in epididymal spermatozoa. A: Controls with the first or second antibody alone showed inconsistent weak staining in the mitochondrial sheath (m). B: SR-BI is localized over the anterior acrosomal segment (aa) and scattered in clumps; the mitochondrial sheath is also labeled. C: The anterior acrosomal segment is strongly SR-BII-positive and is ended by a distinct shape reminiscent of a pair of eyebrows (asterisk) next to the equatorial segment, which itself is not labeled. Magnification, ×980.

hood. In the adult, FC levels decreased from December to March. The profile of the EC levels in the STf was reminiscent of that in the ITf, except that the November-to-December decrease ($P < 0.01$) was significant and there was a significant increase from March to April ($P < 0.02$) followed by a significant decrease from April to May ($P < 0.05$). Serum FC and EC values were near each other and ranged between 80 and 90 mg cholesterol/dl serum and 90 and 104 mg cholesterol/dl, respectively, without showing significant differences.

Studies on adult mink with spontaneous AIO

SR-BI and SR-BII levels in the STf of normal mink and mink with AIO. In **Fig. 8**, for each month studied, the control value was set at 1 and the AIO values were compared with the corresponding controls. SR-BI levels were increased significantly in mink with AIO in February ($P < 0.02$, AIO vs. normal). However, control SR-BI values did not differ significantly from those in mink with AIO in March and July. SR-BII levels were not significantly higher in mink with AIO than in controls in February. However, SR-BII was decreased significantly by March ($P < 0.02$, AIO vs. normal) and increased significantly by July ($P < 0.05$, AIO vs. normal).

FC and EC levels in the STf in normal mink and mink with AIO. There were no significant differences between normal and AIO FC values (**Fig. 9**). However, EC levels tended to be higher in mink with AIO than in normal mink in the 3 months studied, and the difference was significant ($P < 0.02$, AIO vs. normal) by March.

Apoptosis levels measured by cell death detection with ELISA in the cytoplasmic fraction of the STf obtained from adult normal fertile mink and mink with AIO. Apoptosis levels were higher in mink with AIO than in normal mink in February, but the values were not significantly different for any of the months studied (**Fig. 10**).

Serum testosterone levels

Serum testosterone levels were significantly lower in mink with AIO than in normal mink in February and March but not in July (**Table 1**).

DISCUSSION

SR-BI is an integral membrane cell glycoprotein well preserved among mammalian species, given that the predicted protein sequences of hamster, mouse, rat, cow, and human have been reported to nearly 80% identity (48, 49). The SR-BI-immunoreactive band showed a molecular mass of 82 kDa in mink. This observation differs from the report of dimeric (164 kDa) and hetero/oligomeric forms in rat (50, 51) and from that of a "discreet signal with a molecular mass of ~70 kDa" in membrane subfractions of primary cultured, pubertal 20 day old rat Sertoli cells and liver (38).

Cholesterol and apoptosis levels

Our results show that measurements generated with the N-EVAP Nitrogen Evaporator reflect real FC and EC levels and substantiate the data we had obtained previously by TLC (20).

Apoptosis levels measured by ELISA in whole testis extracts (52) and in enriched STfs (our unpublished results) showed a 2-fold increase in March and July in normal mink. The phagocytosis of massive numbers of apoptotic cells entails a cholesterol buildup that results in increased EC levels by March and April, whereas the decreased EC levels in July reflect reduced cholesterol amounts originating from fewer apoptotic cells remaining during this period. The observation of infrequent apoptotic figures in February in mink testis sections despite the report that apoptosis-mediated germ cell death accounts for half of the cell loss in normal testis (17, 18) implies a rapid removal and disposal by Sertoli cells. Moreover, our observation that low EC levels in February prevailed suggests a contribution of SR-BI/SR-BII to the removal of cholesterol-containing germ cells from the tubules back to the liver for the reverse transport of peripheral cholesterol during periods of spermatogenic activity. In normal mink, EC levels were lowest when SR-BI and SR-BII expression were both high, but the levels increased when only one isoform was predominant in the tubules. This suggests that the maintenance of low EC levels requires both isoforms and that each one influences cholesterol in a distinct manner in normal tubules. However, impaired clearance of cholesterol-containing apoptotic cells by Sertoli cells deregulates cholesterol homeostasis and results in increased EC levels in mink tubules with AIO, in which a significant

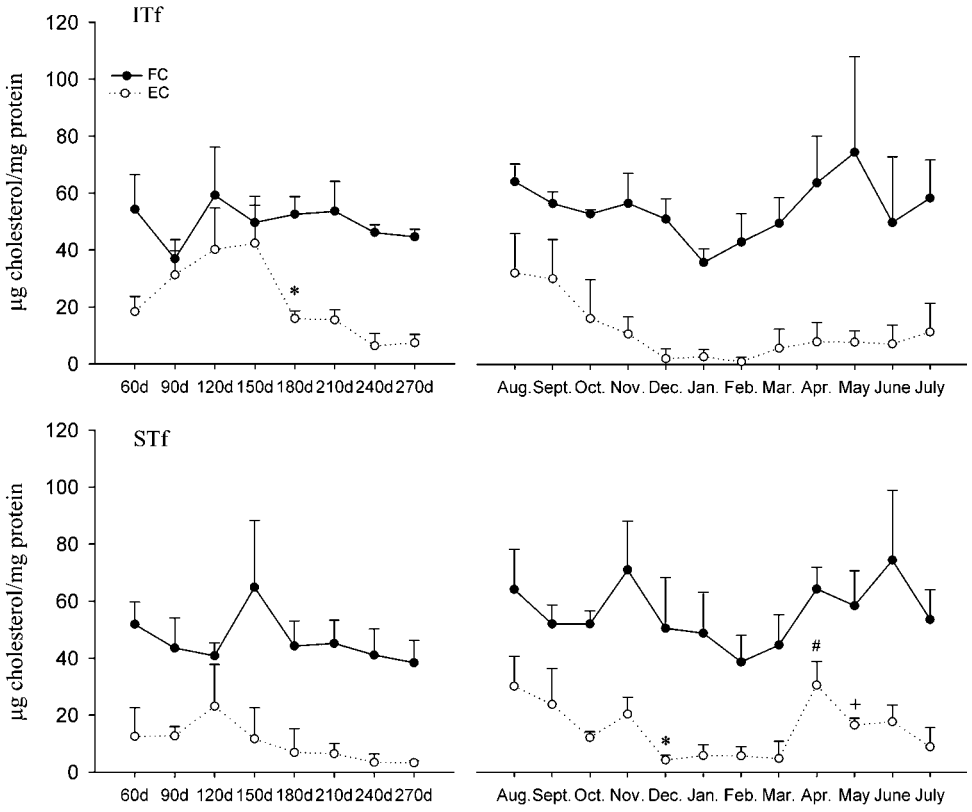

Fig. 7. Free cholesterol (FC) and esterified cholesterol (EC) levels in normal STf and ITf and serum. FC (closed circles) and EC (open circles) are expressed in µg cholesterol/mg total protein for the ITf and STf. The values shown are means ± SEM of three independent experiments. In the ITf (top), FC levels from 120 to 270 day old mink were not significantly higher than those from 90 day old animals. However, EC levels decreased significantly (* $P < 0.01$) from 150 to 180 days. In adult mink, FC and EC levels were both lower, but not significantly, in January and February than during the remainder of the annual reproductive cycle. In the STf (bottom), FC and EC levels were not significantly different during development. However, in the adult, EC but not FC showed significant differences during the annual reproductive cycle. EC levels decreased significantly from November to December (* $P < 0.01$), they increased from March to April ($^{\#}$ $P < 0.02$), and finally, they decreased from April to May ($^{+}$ $P < 0.05$).

EC increase was accompanied by a decrease in SR-BII but not SR-BI in March. This observation is consistent with the report that experimental hepatic overexpression of SR-BI induces a significant diminution of HDL cholesterol (53).

We show here the first measurements of SR-BI and SR-BII in individual compartments rather than in whole testis extract. Regarding the tubular compartment, the results with vimentin, a marker for Sertoli cells, showed that the concentration of vimentin-containing Sertoli cells in STf samples was lowest during periods when spermatogenesis was near completion, although the total Sertoli cell number per testis remained constant regardless of spermatogenic activity through the annual reproductive cycle. In addition, the vimentin concentration profiles during the development and annual cycle were similar to those in SR-BI. Therefore, SR-BI variations are concomitant with those in the proportion of Sertoli cells relative to the germ cell

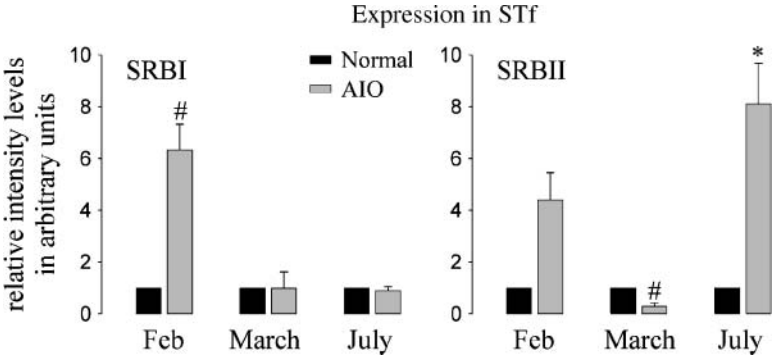

Fig. 8. Measurements of SR-BI and SR-BII levels in the STf in normal fertile adult mink and in mink with autoimmune orchitis (AIO) in February, March, and July. The SR-BI levels were very significantly increased in mink with AIO in February ($\#P < 0.02$, AIO vs. normal) but not in March and July. SR-BII levels were significantly decreased by March ($\#P < 0.02$, AIO vs. normal) but increased by July ($*P < 0.05$, AIO vs. normal). The values shown are the mean ± SEM of three independent experiments.

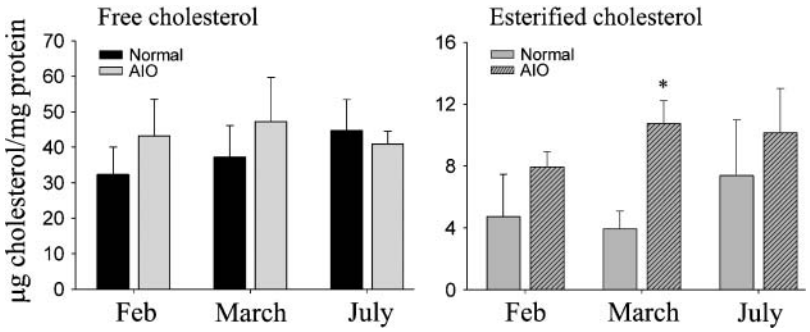

Fig. 9. FC and EC levels in the STf in normal fertile adult mink and mink with AIO in February, March, and July. Normal versus AIO mink FC levels (expressed in µg cholesterol/mg total protein) were not significantly different in February, March, and July, but the EC levels tended to be higher in mink with AIO than in normal mink. In March, the difference was significant (* $P < 0.02$, AIO vs. normal). The values shown are means ± SEM of three independent experiments.

population in the sample. This does not exclude the possibility that the profile of variations in vimentin or in SR-BI indicates a specific change in vimentin and SR-BI gene expression. The predominance of SR-BI from July to February and of SR-BII from January to June suggests that an increase in SR-BII causes a restriction in SR-BI expression in normal mink tubules. During AIO, however, the feedback mechanism responsible for the expression in tandem of each isoform is perturbed, as shown by the observations that SR-BI and SR-BII expression was concurrent and that SR-BI increased in February but SR-BII increased in July, opposite of the normal measurements.

SR-BI/SR-BII expression and apoptosis levels

Our results show that the peak in apoptosis levels reported in whole testis extracts (52) and tubule-enriched fractions (our unpublished data) in March corresponds to increased SR-BII levels, whereas the peak in apoptosis recorded in July corresponds to high SR-BI levels. This could suggest the involvement of a distinct isoform in the removal of distinct generations of germ cells in normal tubules. However, our observation that increased SR-BI and/or SR-BII levels were not accompanied by significant increases in apoptosis in mink with AIO in February and July agrees with the reports that the expression of individual receptors (54–56) and the genetic deletion of scavenger receptor A (57) only produce minimal effects on the uptake of apoptotic cells in culture. Our results suggest that other multiligands besides SR-BI/SR-BII are involved in apoptosis and that this process is not causally related to SR-BI expression in testis. However, our results contrast with the report that injection of rat SR-BI into seminiferous tubules causes an increase in the number of apoptotic cells identified with the Terminal deoxynucleotidyl Transferase Biotin-dUTP Nick End Labeling (TUNEL) method in mice (37). The TUNEL measures apoptotic cells not engulfed and remaining in tubules (i.e., clearance by Sertoli cells), whereas ELISA measurements reflect real apoptosis levels. Other studies have reported an increase in in situ end labeling (ISEL)-positive apoptotic germ cells in the tubules during experimental AIO in rat (58). More importantly, our finding of increased numbers of apostain-labeled apoptotic germ cells in mink tubules in which apoptosis levels measured by ELISA were not increased is proof that cell clearance is impaired during spontaneous AIO in mink (our unpublished data). Apoptosis is characterized by the appearance of plasma membrane blebs that have been shown to express externalized phosphatidylserine and to constitute sites for C1q and C-reactive protein binding, both of which are events connected with the noninflammatory clearance of cellular debris (59). The finding that phagocytosis of apoptotic germ cells was inhibited by liposomes containing phosphatidylserine (60) and/or by anti-SR-BI antibody provides strong support for the conclusion that SR-BI acts as a phosphatidylserine receptor (38).

Here, we show deregulated SR-BI and SR-BII expression in mink testis with AIO, which could alter the bleb recognition of dying germ cells and lead to impaired clearance

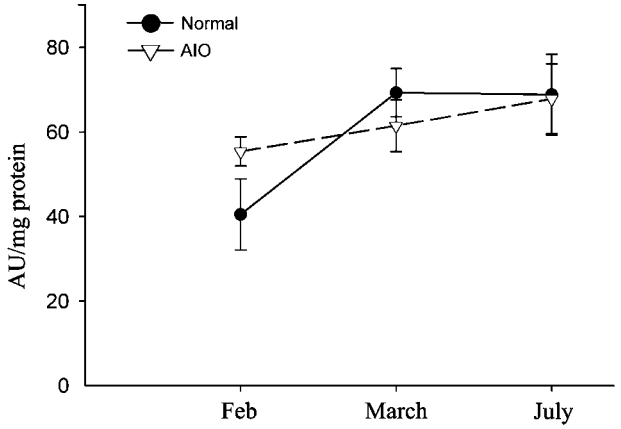

Fig. 10. Apoptosis levels measured by cell death detection. ELISA in the cytoplasmic fraction of STf from normal fertile mink and mink with AIO. The data are expressed as optical density at 410 nm, and the values represent means ± SEM of measurements performed in six different animals per experimental condition. Apoptosis levels in fertile and infertile STf were not significantly different.

TABLE 1. Serum testosterone levels in normal adult mink and mink with AIO

Month	Normal	AIO
February	9.58 ± 1.74 (n = 7)	1.93 ± 0.52 (n = 6)[a]
March	1.65 ± 0.62 (n = 8)	0.33 ± 0.09 (n = 9)[b]
July	0.64 ± 0.08 (n = 4)	0.44 ± 0.09 (n = 4)

AIO, autoimmune orchitis. Testosterone levels in serum measured by ELISA are expressed in ng/ml serum. The values shown are means ± SEM, and the number of animals in which the measurements were performed is indicated in parentheses.

[a] $P < 0.03$, AIO versus normal in February.

[b] $P < 0.05$, AIO versus normal in March.

by Sertoli cells. A deficit in SR-BI-mediated recognition of the nuclear antigens that have been shown to redistribute in blebs and apoptotic bodies (61) could favor intolerance to self proteins. The observation here that an increase in SR-BI or SR-BII was accompanied by minimal effects on apoptosis levels supports the notion that the recognition and phagocytosis of apoptotic cells are distinct physiological events and that the engulfment of apoptotic cells by Sertoli cells is only partly SR-BI-dependent.

The distribution of SR-BI and SR-BII

The interstitial compartment. Our finding of SR-BI at the mink Leydig cell plasma membrane agrees with similar findings in rat (62, 63). However, the discrepancy between our observation of a strong rather than "a very weak SR-BI staining" and "barely detectable" (62) SR-BI levels likely stems from the fact that mink Leydig cells are rich (64), whereas rat Leydig cells are poor, in cholesteryl ester-containing lipid droplets (65) and in the use endogenous, not exogenous, blood-borne HDL or LDL cholesterol for the purpose of testosterone production (62).

The seminiferous tubules. Our observation of SR-BI localized to mink Sertoli cells agrees with the finding of the receptor protein and mRNA (39) and of SR-BI as a phagocytosis-inducing phospholipid phosphatidylserine receptor in rat Sertoli cells (37). In addition, our detection of SR-BI on testicular cell and spermatozoan surfaces and of SR-BII on the inner acrosome overlying the nucleus is consistent with the report of ~70% of SR-BI on the cell surface and ~80–90% of SR-BII around the Chinese hamster ovary cell nucleus (66). In addition, our localization of SR-BI to mink Sertoli cell junctional membranes, except when it accumulates in the trunk of the cell during stage X of the cycle of the seminiferous epithelium, entails factors modifying its location to adapt to the physiological activities of the cell. This view is supported by the report of decreased SR-BI mRNA expression during stages I–VI in rat (39). In addition, SR-BI was reported to modify the structure of the membrane (67, 68) and the distribution of cholesterol within the membrane (69, 70). We showed that cholesterol accumulates in germ cell membranes (71), at the tight junctions of Sertoli cells (72–74), and within testicular cells (74). SR-BI/SR-BII-mediated selective lipid uptake in testicular cell membrane segments could modify the membrane fluidity causing local concentration of signaling proteins for signal transduction, which would in turn influence cell-cell interactions. In particular, spermatocyte translocation from one side to the other of the blood-testis barrier during stage X requires Sertoli cell junction plasticity while the spermatids release into the lumen, and the engulfment by Sertoli cells of lipid-containing residual bodies involves the intracellular management of cholesterol. A change in the scavenger receptor location could influence both of these events, because the "selective uptake of lipids by SR-BI and SR-BII correlates with the surface expression of SR-BI and SR-BII rather than with the rate at which the two receptors accumulate HDL intracellularly" (66, 75). The lack of a C-terminal leucine amino acid decreased the surface expression of SR-BI in mouse hepatocytes, and the three C-terminal amino acids required for binding PDZK1 are lacking in SR-BII (76). Interestingly, hormone-sensitive lipase (20) and SR-BI expression are both upregulated in the tubules during stage X.

In conclusion, cholesterol homeostasis and SR-BI expression are deregulated, but apoptosis levels are unchanged, in tubules with AIO. These results suggest that SR-BI and SR-BII expression favors the maintenance of low EC levels and that the predominance of only one isoform is associated with the accumulation of EC but not with apoptosis in the tubules.

The authors express their sincere gratitude to Dr. Marshall E. Bloom from the Laboratory of Persistent Viral Diseases (National Institute of Allergy and Infectious Diseases, National Institutes of Health, Hamilton, MT) for his generous and invaluable gift of rabbit anti-mink IgG. The authors are immensely indebted and grateful to Dr. Lise Bernier (IRCM) for her guidance in the cholesterol measurements. This work was supported in part by Natural Sciences and Engineering Research Council of Canada Grant OGP0041653 and by a Population Council ICMC grant to R-M.P. and by NSERC Grant OGP0194652 to M.L.V. M.L.V. was also funded by a scholarship from Les Fonds de la Recherche en Santé du Québec.

REFERENCES

1. Ramirez-Torres, M. A., A. Carrera, and M. Zambrana. 2000. High incidence of hyperestrogenemia and dyslipidemia in a group of infertile men. *Ginecol. Obstet. Mex.* **68:** 224–229.
2. Osuga, J., S. Ishibashi, T. Oka, H. Yagyu, R. Tozawa, A. Fujimoto, F. Shionoiri, N. Yahagi, F. B. Kreamer, O. Tsutsumi, et al. 2000. Targeted disruption of hormone-sensitive lipase results in male sterility and adipocyte hypertrophy, but not in obesity. *Proc. Natl. Acad. Sci. USA.* **97:** 787–792.
3. Chung, S., S. P. Wang, L. Pan, G. A. Mitchell, J. M. Trasler, and L. Hermo. 2001. Infertility and testicular defects in hormone-sensitive lipase-deficient mice. *Endocrinology.* **142:** 4272–4281.
4. Vallet-Erdtmann, V., G. Tavernier, J. A. Contreras, A. Mairal, C. Rieu, A-M. Touzalin, C. Holm, B. Jégou, and D. Langin. 2004. The testicular form of hormone-sensitive lipase HSL_{tes} confers rescue of male infertility in HSL-deficient mice. *J. Biol. Chem.* **279:** 42875–42880.
5. Wechsler, A., A. Brafman, M. Shafir, M. Heverin, H. Gottlieb, G. Damari, S. Gozlan-Kelner, I. Spivak, O. Moshkin, E. Fridman, et al. 2003. Generation of viable cholesterol-free mice. *Science.* **302:** 2087.
6. Rodemer, C., T. P. Thai, B. Brugger, T. Kaercher, H. Werner, K. A. Nave, F. Wieland, K. Gorgas, and W. W. Just. 2003. Inactivation of ether lipid biosynthesis causes male infertility, defect in eye development and optic nerve hypoplasia in mice. *Hum. Mol. Genet.* **12:** 1881–1895.
7. Selva, D. M., V. Hirsh-Reinshagen, B. Gurgess, S. Zhou, J. Chan, S. McIsaac, M. R. Hyden, G. L. Hammon, A. W. Vogl, and C. L. Wellington. 2004. The ATP-binding cassette transporter 1 mediates lipid efflux from Sertoli cells and influences male fertility. *J. Lipid Res.* **45:** 1040–1050.
8. Sugkraroek, P., M. Kates, A. Leader, and N. Tanphaichitr. 1991. Level of cholesterol and phospholipids in freshly ejaculated sperm and Percoll-gradient-pelleted sperm from fertile and unexplained infertile men. *Fertil. Steril.* **55:** 820–827.
9. Steinberger, E., A. Root, M. Fisher, and K. D. Smith. 1973. The role of androgens in the initiation of spermatogenesis in man. *Clin. Endocrinol. Metab.* **37:** 746–749.
10. McLachland, R. I., N. G. Wreford, L. O'Donnell, D. M. de Kretser, and D. M. Robertson. 1996. The endocrine regulation of spermatogenesis: independent roles for testosterone and FSH. *J. Endocrinol.* **148:** 1–9.

11. Fofana, M., J-C. Maboundou, J. Bocquet, and D. Le Goff. 1996. Transfer of cholesterol between high density lipoproteins and cultured rat Sertoli cells. *Biochem. Cell Biol.* **74:** 681–686.
12. Fofana, M., C. Travert, C. Carreeau, and D. LeGoff. 2000. Evaluation of cholesteryl ester transfer in the seminiferous tubule cells of immature rats *in vivo* and *in vitro*. *J. Reprod. Fertil.* **118:** 79–83.
13. Pelletier, R-M., and S. W. Byers. 1992. The blood-testis barrier and Sertoli cell junctions: structural considerations. *Microsc. Res. Tech.* **20:** 3–33.
14. Pelletier, R-M. 2004. The tight junction in the testis. *In* Recent Research in Development and Endocrinology. S. G. Pandalai, editor. Transworld Research Network, Trivandrum, India. 29–51.
15. Setchell, B. P., and G. M. H. Waites. 1975. The Blood-Testis Barrier. American Physiological Society, Washington, DC. 143–172.
16. Wiebe, J. P., and K. S. Tilbe. 1979. *De novo* synthesis of steroids (from acetate) by isolated rat Sertoli cells. *Biochem. Biophys. Res. Commun.* **89:** 1107–1113.
17. Huckins, C. 1978. The morphology and kinetics of spermatogonial degeneration in normal adult rats: an analysis using a simplified classification of the germinal epithelium. *Anat. Rec.* **190:** 905–926.
18. Kerr, J. B. 1992. Spontaneous degeneration of germ cells in normal rat testis: assessment of cell types and frequency during the spermatogenic cycle. *J. Reprod. Fertil.* **95:** 825–830.
19. Kabbaj, O., C. Holm, M. L. Vitale, and R-M. Pelletier. 2001. Expression, activity and subcellular localization of testicular hormone-sensitive lipase (HSL) during postnatal development in the guinea pig. *Biol. Reprod.* **65:** 601–612.
20. Kabbaj, O., S. R. Yoon, C. Holm, J. Rose, M. L. Vitale, and R-M. Pelletier. 2003. Relationship of the hormone sensitive lipase (HSL)-mediated modulation of cholesterol metabolism in individual compartments of the testis to serum pituitary hormone and testosterone concentrations in a seasonal breeder, the mink (*Mustela vison*). *Biol. Reprod.* **68:** 722–734.
21. Wellington, C. L., E. C. Walker, A. Suarez, A. Kwok, N. Bissada, R. Singaraja, Y-Z. Yang, L. H. Zhang, E. James, J. E. Wilson, et al. 2002. ABCA1 mRNA and protein distribution patterns predict multiple different roles and levels of regulation. *Lab. Invest.* **82:** 273–283.
22. Arenas, M. I., M. V. T. Lobo, E. Caso, L. Huerta, R. Paniagua, and M. A. Martin-Hidalgo. 2004. Normal and pathological human testes express hormone-sensitive lipase and the lipid receptors CLA-1/CD36. *Hum. Pathol.* **35:** 34–42.
23. Temel, R. E., B. Trigatti, R. B. DeMattos, S. Azhar, and D. L. Williams. 1997. Scavenger receptor class B, type I (SR-BI) is the major route for the delivery of high density lipoprotein cholesterol to the steroidogenic pathway in cultured mouse adrenocortical cells. *Proc. Natl. Acad. Sci. USA.* **94:** 13600–13605.
24. Kozarsky, K. F., M. H. Donahee, A. Rigotti, S. N. Iqbal, E. R. Edelman, and M. Krieger. 1997. Overexpression of the HDL receptor SR-BI alters plasma HDL and bile cholesterol levels. *Nature.* **387:** 414–417.
25. Ji, Y., N. Jian, Y. Wang, Y. Sun, M. L. Moya, M. C. Phillips, G. H. Rothblat, J. B. Swaney, and A. R. Tall. 1997. Scavenger receptor BI promotes high density lipoprotein-mediated cellular cholesterol efflux. *J. Biol. Chem.* **272:** 20982–20985.
26. Trigatti, B., H. Rayburn, M. Vinals, A. Braun, H. Miettinen, M. Penman, M. Hertz, M. Schrenzez, L. Amigo, A. Rigott, et al. 1999. Influence of the high density lipoprotein receptor SR-BI on reproductive and cardiovascular pathophysiology. *Proc. Natl. Acad. Sci. USA.* **96:** 9322–9327.
27. Webb, N. R., W. J. S. de Villiers, P. M. Connell, F. C. de Beer, and D. R. van der Westhuyzen. 1997. Alternative forms of the scavenge receptor BI (SR-BII). *J. Lipid Res.* **38:** 1490–1495.
28. Mulcahy, J. V., D. R. Riddell, and J. S. Owen. 2004. Human scavenger receptor class B type II (SR-BII) and cellular cholesterol efflux. *Biochem. J.* **277:** 741–747.
29. Babitt, J., B. Trigatti, A. Rigotti, E. J. Smart, R. G. Anderson, S. Xu, and M. Krieger. 1997. Murine SR-BI, a high density lipoprotein receptor that mediates selective lipid uptake, is N-glycosylated and fatty acetylated and colocalizes with plasma membrane caveolae. *J. Biol. Chem.* **272:** 13242–13249.
30. Webb, N. R., P. M. Connell, G. A. Graf, E. J. Smart, W. J. S. de Villiers, F. C. de Beer, and D. R. van der Westhuyzen. 1998. SR-BII, an isoform of the scavenger receptor BI containing an alternate cytoplasmic tail, mediates lipid transfer between high density lipoprotein and cells. *J. Biol. Chem.* **273:** 15241–15248.
31. Graf, G. A., S. V. Matveev, and E. J. Smart. 1999. Class B scavenger receptors, caveolae and cholesterol homeostasis. *Trends Cardiovasc. Med.* **9:** 221–225.
32. Fielding, C. J., and P. E. Fielding. 2000. Cholesterol and caveolae: structural and functional relationships. *Biochim. Biophys. Acta.* **1529:** 210–222.
33. Fielding, C. J. 2001. Caveolae and signaling. *Curr. Opin. Lipidol.* **12:** 281–287.
34. Voisin, G. A., and F. Toullet. 1968. Étude sur l'orchite aspermatogénique autoimmune et les autoantigènes des spermatozoïdes chez le cobayes. *Ann. Inst. Pasteur (Paris).* **114:** 727–755.
35. Tung, K. S. K. 1998. Autoimmune disease of the testis and the ovary. *In* The Autoimmune Diseases. Academic Press, New York. 687–704.
36. Schuppe, H-C., and A. Meinhardt. 2005. Immune privilege and inflammation of the testis. *In* Immunology of Gametes and Embryo Implantation: Immunology of the Male Reproductive System, Male Infertility and Contraception. U. R. Marker, editor. Karger, Basel, Switzerland. 1–14.
37. Kawasaki, Y., A. Nakagawa, K. Nagaosa, A. Shiratsuchi, and Y. Nakanishi. 2002. Phosphatidylserine binding of class B scavenger receptor type I, a phagocytosis receptor of testicular Sertoli cells. *J. Biol. Chem.* **277:** 27559–27566.
38. Shiratsuchi, A., Y. Kawasaki, M. Ikemoto, H. Arai, and Y. Nakanishi. 1999. Role of class B scavenger receptor type I in phagocytosis of apoptotic rat spermatogenic cells by Sertoli cells. *J. Biol. Chem.* **274:** 5901–5908.
39. Nakagawa, A., K. Nagaosa, T. Hirose, K. Tsuda, K. Hasegawa, A. Shiratsuchi, and Y. Nakanishi. 2004. Expression and function of class B scavenger receptor type I on both apical and basolateral sides of the plasma membrane of polarized testicular Sertoli cells of the rat. *Dev. Growth Differ.* **46:** 283–298.
40. Pelletier, R-M. 1986. Cyclic formation and decay of the blood-testis barrier in the mink (*Mustela vison*): a seasonal breeder. *Am. J. Anat.* **175:** 91–117.
41. Ing, R. M. Y., S-X. Wang, A. M. Brennecke, and W. R. Jones. 1985. An improved indirect enzyme-linked immunosorbent assay (ELISA) for the detection of antisperm antibodies. *Am. J. Reprod. Immunol.* **8:** 15–19.
42. Benet-Rubinat, J. M., P. Martinez, W. A. Lepp, J. Egozcue, P. Andolz, and M. A. Bielsa. 1991. Detection of induced anti-sperm antibodies by an improved enzyme-linked immunosorbent assay. *Int. J. Fertil.* **36:** 48–56.
43. Bradford, M. M. 1976. A rapid and sensitive method for the quantitation of microgram quantities of protein utilizing the principle of protein-dye binding. *Anal. Biochem.* **72:** 248–254.
44. Herrada, G., and D. J. Wolgemuth. 1997. The mouse transcription factor Stat4 is expressed in haploid male germ cells and is present in the perinuclear theca of spermatozoa. *J. Cell Sci.* **110:** 1543–1553.
45. Rigotti, A., B. L. Trigatti, M. Penman, H. Reyburn, J. Herz, and M. Krieger. 1997. A targeted mutation in the murine gene encoding the high density lipoprotein (HDL) receptor scavenger receptor class B type I reveals its key role in HDL metabolism. *Proc. Natl. Acad. Sci. USA.* **94:** 12610–12615.
46. Pelletier, R-M. 1988. Cyclic modulation of the Sertoli cell junctional complexes in a seasonal breeder: the mink (*Mustela vison*). *Am. J. Anat.* **183:** 68–102.
47. Franz, H. R., and L. C. Ellis. 2001. Duration of spermatogenesis and spermatozoan transport in the mink (*Mustela vison*). *Norw. J. Agric. Sci.* **9:** 122–127.
48. Krieger, M. 1999. Charting the fate of the "good cholesterol": identification and characterization of the high-density lipoprotein receptor SR-BI. *Annu. Rev. Biochem.* **68:** 523–558.
49. Williams, D., M. A. Connelly, R. E. Temel, S. Swanakar, M. C. Phillips, M. de la Llera-Moya, and G. H. Rothblat. 1999. Scavenger receptor BI and cholesterol trafficking. *Curr. Opin. Lipidol.* **10:** 329–339.
50. Azhar, S., A. Nomoto, and E. Reaven. 2002. Hormonal regulation of microvillar channel formation. *J. Lipid Res.* **43:** 861–871.
51. Reaven, E., Y. Cortez, S. Leers-Sucheta, A. Namoto, and S. Azhar. 2004. Dimerization of the scavenger receptor class B type I: formation, function, and localization in diverse cells and tissues. *J. Lipid Res.* **45:** 513–528.
52. Blottner, S., H. Roelands, A. H. Wagner, and U. D. Wenzel. 1999. Testicular mitosis, meiosis and apoptosis in mink (*Mustela vison*) during breeding and non-breeding seasons. *Anim. Reprod. Sci.* **57:** 237–249.
53. Kozarsky, K. F., M. H. Donahee, J. M. Glick, M. Krieger, and D. J. Rader. 2000. Gene transfer and hepatic overexpression of the HDL receptor SR-BI reduces atherosclerosis in the cholesterol-fed LDL receptor-deficient mouse. *Arterioscler. Thromb. Vasc. Biol.* **20:** 721–727.

54. Navazo, M. D., L. Daviet, J. Savill, Y. Ren, L. L. Leung, and J. L. McGregor. 1996. Identification of a domain (155–183) on CD36 implicated in the phagocytosis of apoptotic neutrophils. *J. Biol. Chem.* **271:** 15381–15385.
55. Devitt, A., O. D. Moffatt, C. Raykundalia, J. D. Capra, D. L. Simmons, and C. D. Gregory. 1998. Human CD14 mediates recognition and phagocytosis of apoptotic cells. *Nature.* **392:** 505–509.
56. Mamon, Y., C. Broccardo, O. Chambenoir, M. F. Luciani, F. Toti, S. Chaslin, J. M. Fressinet, P. F. Devaux, J. McNeish, D. Marguet, et al. 2000. ABCA1 promotes engulfment of apoptotic cells and transbilayer redistribution of phosphatidylserine. *Nat. Cell Biol.* **2:** 399–406.
57. Platt, N., H. Suzuki, Y. Kurihara, T. Kodama, and S. Gordon. 1996. Role of the class A macrophage scavenger receptor in the phagocytosis of apoptotic thymocytes in vitro. *Proc. Natl. Acad. Sci. USA.* **93:** 12456–12460.
58. Morales, C. R., Y. Clermont, and L. Hermo. 1985. Nature and function of endocytosis in Sertoli cells of the rat. *Am. J. Anat.* **173:** 203–217.
59. Korb, L. C., and J. M. Ahearn. 1997. C1q binds directly and specifically to surface blebs of apoptotic human keratinocytes: complement deficiency and systemic lupus erythematosus revisited. *J. Immunol.* **158:** 4525–4528.
60. Shiratsuchi, A., M. Umeda, Y. Ohba, and Y. Nakanishi. 2006. Recognition of phosphatidylserine on the surface of apoptotic spermatogenic cells and subsequent phagocytosis by Sertoli cells. *J. Biol. Chem.* **272:** 2354–2358.
61. Henson, P. M., D. L. Bratton, and V. A. Fadok. 2001. The phosphatidylserine receptor: a crucial molecular switch? *Nat. Rev. Mol. Cell Biol.* **2:** 627–633.
62. Reaven, E., L. Zhan, A. Nomoto, S. Leers-Sucheta, and S. Azhar. 2000. Expression and microvillar localization of scavenger receptor class B, type I (SR-BI) and a selective cholesteryl ester uptake in Leydig cells from rat testis. *J. Lipid Res.* **41:** 343–356.
63. Eckhardt, E. R. M., L. Cai, J. Shetty, Z. Zhao, A. Szanto, N. R. Webb, and D. R. van der Westhuyzen. 2006. HDL endocytosis by scavenger receptor SR-BII is clathrin-dependent and requires a carboxy-terminal dileucine motif. *J. Biochem. (Tokyo).* **281:** 4348–4353.
64. Sundqvist, C., L. C. Ellis, and A. Bartke. 1988. Reproductive endocrinology of the mink (*Mustela vison*). *Endocr. Rev.* **9:** 247–266.
65. Benton, L., L-X. Shan, and M. P. Hardy. 1995. Differentiation of adult Leydig cells. *J. Steroid Biochem. Mol. Biol.* **53:** 61–68.
66. Eckhardt, E. R. M., L. Cai, N. R. Webb, and D. R. van der Westhuyzen. 2004. HDL uptake by scavenger receptor SR-BII. *J. Biol. Chem.* **279:** 14372–14381.
67. Reaven, E., S. Leers-Sucheta, A. Nomoto, and S. Azhar. 2001. Expression of scavenger receptor class B type I (SR-BI) promotes microvillar channel formation and selective cholesteryl ester transport in a heterologous and reconstituted system. *Proc. Natl. Acad. Sci. USA.* **98:** 1613–1618.
68. Williams, D., J. S. Wong, and R. L. Hamilton. 2002. SR-BI is required for microvillar channel formation and the localization of HDL particles to the surface of adrenocortical cells *in vivo*. *J. Lipid Res.* **43:** 544–549.
69. de la Llera-Moya, M., G. H. Rothblat, M. A. Connelly, G. Kellner-Weibel, S. W. Sakr, M. C. Phillips, and D. L. Williams. 1999. Scavenger receptor BI (SR-BI) mediates free cholesterol flux independently of HDL tethering to the cell surface. *J. Lipid Res.* **40:** 575–580.
70. Kellner-Weibel, G., M. de la Llera-Moya, M. A. Connelly, G. Stoudt, A. E. Christian, M. P. Haynes, D. L. Williams, and G. H. Rothblat. 2000. Expression of scavenger receptor BI in COS-7 cells alters cholesterol content and distribution. *Biochemistry.* **39:** 221–229.
71. Pelletier, R-M., and D. S. Friend. 1983. Development of membrane differentiations in the guinea pig spermatid during spermiogenesis. *Am. J. Anat.* **167:** 119–141.
72. Pelletier, R-M., and D. S. Friend. 1983. The Sertoli cell junctional complex: structure and permeability to filipin in the neonatal and adult guinea pig. *Am. J. Anat.* **168:** 213–228.
73. Pelletier, R-M., and D. S. Friend. 1986. Sertoli cell junctional complexes in gossypol-treated neonatal and adult guinea pigs. *J. Androl.* **7:** 127–139.
74. Pelletier, R-M., and M. L. Vitale. 1994. Filipin vs enzymatic localization of cholesterol in guinea pig, mink, and mallard duck testicular cells. *J. Histochem. Cytochem.* **42:** 1539–1554.
75. Savill, J., and V. Fadok. 2000. Corpse clearance defines the meaning of cell death. *Nature.* **407:** 784–788.
76. Silver, D. 2002. A carboxyl-terminal, PDZ-interacting domain of scavenger receptor B, type I is essential for cell surface expression in liver. *J. Biol. Chem.* **277:** 34042–34047.